Investigation of Donor-Acceptor Interactions: A Charge Decomposition Analysis Using Fragment Molecular Orbitals

Stefan Dapprich and Gernot Frenking*

Fachbereich Chemie, Philipps-Universität Marburg, Hans-Meerwein-Strasse, D-35032 Marburg, Germany

Received: December 8, 1994; In Final Form: March 13, 1995[⊗]

A partitioning scheme for analyzing donor-acceptor interactions in a complex is proposed. The charge decomposition analysis (CDA) constructs the wave function of the complex in terms of the linear combination of the donor and acceptor fragment orbitals (LCFO). Three terms are then calculated for each LCFO orbital of the complex: (i) the charge donation d given by the mixing of the occupied orbitals of the donor and the unoccupied orbitals of the acceptor; (ii) the back donation b given by the mixing of the occupied orbitals of the acceptor and the unoccupied orbitals of the donor; (iii) the charge depletion from the overlapping area (charge polarization) r given by the mixing of the occupied orbitals of donor and acceptor. The sum of the three contributions gives the total amount of donation, back donation and charge polarization in the complex. The CDA is performed for canonical orbitals at HF/6-31G(d) and for natural orbitals at MP2/6-31G(d) for the complexes H_3BCO, H_3BNH_3, $W(CO)_6$, $Ag(CO)^+$, and $Au(CO)^+$. To investigate the basis set dependence of the results, additional calculations are carried out using a TZ2P basis set. Strong electron donation OC → BH_3 (0.550 e) and significant back donation H_3B → CO (0.253 e) are calculated at MP2/6-31G(d) for H_3-BCO. Strong electron donation H_3N → BH_3 (0.382 e) but no back donation H_3B → NH_3 is predicted at MP2/6-31G(d) for H_3BNH_3. A comparable magnitude of donation (0.315 e) and back donation (0.233 e) is calculated at MP2/6-31G(d) for $W(CO)_6$. The electron donation is clearly larger (0.330 and 0.282 e) than the back donation (0.016 and 0.089 e) for $Ag(CO)^+$ and $Au(CO)^+$, respectively. The calculated charge polarization is quite large. It is −0.272 e for H_3BCO, −0.367 e for H_3BNH_3, −0.278 e for $W(CO)_6$, −0.062 e for $Ag(CO)^+$, and −0.190 e for $Au(CO)^+$ (all values at MP2/6-31G(d)). Very similar values are calculated at MP2/TZ2P. The results of the CDA method are compared with qualitative MO interaction diagrams. The CDA can be used as a quantitative expression of the Dewar-Chatt-Duncanson model.

Introduction

Ab initio electronic structure calculations yield the electronic energy and the wave function of a molecular system in a particular electronic state. The wave function itself is not very suitable for interpretation, since it is a function of the coordinates of all electrons. Yet chemists need more simplified notions and characteristics of the wave function in order to gain insight into the electronic structure of molecules and to predict chemical reactivity and other properties. A much clearer picture is provided by the electron density,[1] which is a function of only three coordinates.

Much work has been done in the field of population analyses to assign a discrete charge to an atom in a molecule.[2] In the approaches of Mulliken,[3] Löwdin,[4] Roby,[5] Mayer,[6] Cioslowski,[7] among others,[2] the electron density is projected onto some reference basis set. However, there are some problems with this scheme,[8] because in these approaches the reference basis set is directly related to the AO basis set used in the actual calculation. Davidson[9] proposed a projection of the density onto a minimal basis set, and Weinhold[10] and co-workers derived atomic natural orbitals to reduce the basis set dependence to some degree. The topological analysis of the wave function provides a remedy for the above problem. In the scheme of Bader,[11] the space is divided into loges (atomic basins) that enclose the atoms and the overall charge within a particular loge is assigned to the corresponding atom. There are some disadvantages of this approach: the numerical integration is costly, and there is the possibility of the existence of "empty" loges which are not associated with any atom.[12]

To interpret changes in the electronic structure during the formation of a chemical bond, one has the choice between several procedures. The density difference can be used to locate ranges of charge depletion and charge concentration. A related scheme uses the calculation of the Laplacian $\nabla^2\varrho(\mathbf{r})$ of the density distribution $\varrho(\mathbf{r})$, which determines the regions in space wherein electronic charge is locally concentrated and depleted.

A very important field of chemical research is the application of theoretical models to interpret chemical bonding in transition metal complexes. The interaction between the transition metal and ligands in transition-metal complexes has often been interpreted by crystal field theory, emphasizing the electrostatic nature of the interaction. A more sophisticated approach considers orbital mixing, which stresses the process of charge transfer. The Dewar-Chatt-Duncanson[13] (DCD) model especially falls into this category. The DCD has often been used as a semiempirical basis for the interpretation of metal-ligand interaction. This scheme considers two main factors, the σ-donating interactions from the ligands to the metal and the π back donation from the metal to the ligands. The term "donation" does not necessarily mean a charge-transfer interaction, it rather corresponds to an overall reorganization of electronic charge including polarization, exchange repulsion, and charge transfer. Several papers appearing in the last few years have focused on the evaluation of the energetic contributions to the bond energy. For example, the analysis of Morokuma[14] and the constrained space orbital variation (CSOV) technique[15a-c] developed by Bagus et al. are two widely applied methods. Blyholder[16] suggested the diatomic energy contribution of particular orbitals using the NDO approximation as a criterion for determining the σ and π contributions to the bonding in

[⊗] Abstract published in *Advance ACS Abstracts,* May 15, 1995.

0022-3654/95/2099-9352$09.00/0

transition-metal carbonyls. Very recently, Glendening and Streitwieser published the so-called natural energy decomposition analysis (NEDA).[17]

We have developed a tool for correlating the wave function to this traditional viewpoint of "donation" and "back donation", which characterizes single orbitals as well as the whole complex. Within this method, the interaction between two fragments A and B is partitioned into three terms: electron donation from A to B, electron donation from B to A, and reorganization due to electron−electron repulsion in the bonding region. The method is based upon an earlier approach by Frenking and Heinrich,[18a] who used the linear combination of fragment orbitals (LCFO) of properly chosen fragments A and B for the interpretation of the interactions in the molecule AB. The transformation matrix (given by the coefficients of the LCFO calculation) between the MOs of the complex AB and the MOs of the noninteracting fragments A and B indicates directly the interactions between A and B in terms of orbital interactions. The interpretation of the interactions using the whole transformation matrix is very complex, because each MO of AB is expressed in terms of orbitals A and B.[18] The complexity increases further when larger than minimal basis sets are used. Therefore, we have used a simpler scheme which gives for each orbital of AB (calculated by the LCFO method) only three contributions: (i) the mixing between the occupied orbitals of A and empty orbitals of B; (ii) the mixing between the occupied orbitals of B and the empty orbitals of A; (iii) the mixing between the occupied orbitals of A and the occupied orbitals of B. The three terms (i)−(iii) may be used to indicate the magnitude of (i) electron donation A → B, (ii) back donation A ← B, and (iii) charge polarization A ↔ B.

We want to emphasize that the present approach is an attempt to extract a model for the interpretation of the chemical bond of donor−acceptor complexes from ab initio wave functions of any theoretical level. Like other models, the CDA method cannot be right or wrong, it can only be useful or not. It is important that the interpretation of a chemical bond using a chemical model is not confused with the *physical* interpretation of chemical bonding. Orbital mixing itself is *not* the origin of binding interactions, because optimal orbitals cannot be improved merely by orbital mixing. However, the mixing of the fragment molecular orbitals for describing the optimal wave function of the complex reflects the electronic interactions of the fragments. A very careful and detailed discussion has been recently given by Davidson et al.,[38a] who analyzed the chemical bonding of $Cr(CO)_6$. We think that theoretical chemistry should not only give accurate data for the geometries, energies, and other observable quantities. A very important part of quantum chemical research should be to interpret the results in terms of qualitative concepts. The calculated wave function can be used for partitioning schemes as mentioned above. The value of the CDA method is that results of ab initio calculations at any level of theory can be understood in terms of the familiar concept of the DCD model. The CDA method can be considered as a quantitative expression of the latter. Another important advantage of the method, which is outlined below, is that it can be used for Hartree−Fock (HF) *and* correlated wave functions. This gives important information about the influence of electron correlation upon the relative magnitude of the donating/back-donating interactions.

We want to point out that the partitioning scheme presented here gives detailed information about the change of the *electronic structure* of AB caused by the interactions between A and B in terms of orbital interactions. There is no direct information given about the *energy* contributions which are associated with the electronic charge reorganization. This is different to the approach by Glendening and Streitwieser,[17] who developed a natural energy decomposition analysis of molecules AB based upon the interactions between fragments A and B. Also the partitioning scheme suggested by Morokuma[16] focuses on the energy components of the fragment interactions. The construction of molecular orbitals in terms of fragment MOs has earlier been employed by Fukui and others.[19] Related schemes to the CDA are the constrained space orbital variation technique (CSOV) suggested by Bagus and interbond population (IBP) devised by Inagaki.[15d−f] In the CSOV method the wave function of the complex is constructed from the molecular orbitals of the ligand and the metal atom. The CSOV technique makes it possible to estimate the energetic contributions of the intraunit and interunit charge donation and polarization and to separate σ and π contributions by imposing different constraints on the orbital variation. Ziegler proposed a similar method based on density functional theory.[15g−h]

After a detailed outline of the method, we discuss the results of the charge decompositon analysis using simple donor−acceptor complexes of main-group elements (H_3BCO and H_3BNH_3) and transition metals ($W(CO)_6$, $Ag(CO)^+$, and $Au(CO)^+$) as examples. We demonstrate the basis set dependency of the method by showing the results using different basis sets.

Outline of the Method

For a closed-shell system the one-electron density function $\varrho(r)$ is defined in the orbital approximation as

$$\varrho(r) = \sum_{i}^{\text{occ}} 2\varphi_i\varphi_i \tag{1}$$

where φ_i are the (real) molecular orbitals of a molecule AB. More generally, the electron density of correlated wave functions can be described by a single determinant of natural orbitals[20] φ_i^{nat} with respective occupation numbers m_i:

$$\varrho(r) = \sum_i m_i\varphi_i^{\text{nat}}\varphi_i^{\text{nat}} \tag{2}$$

Expanded in an arbitrary basis Φ_μ, one can write

$$\varphi_i = \sum_\mu c_{\mu i}\Phi_\mu \tag{3}$$

$$\varrho(r) = \sum_i\sum_\mu\sum_\nu m_i c_{\mu i} c_{\nu i}\Phi_\mu\Phi_\nu \tag{4}$$

Integration over the entire space leads to the number n of electrons

$$n = \sum_i\sum_\mu\sum_\nu m_i c_{\mu i} c_{\nu i}\langle\Phi_\mu|\Phi_\nu\rangle \tag{5}$$

The electronic charge n_i in a molecular orbital φ_i is then given by

$$n_i = \sum_\mu\sum_\nu m_i c_{\mu i} c_{\nu i}\langle\Phi_\mu|\Phi_\nu\rangle = m_i \tag{6}$$

Commonly the functions Φ_μ are atomic orbitals. However, one can choose any other basis set. The basis constructed from fragment molecular orbitals derived from properly chosen fragments A and B,[21] which are taken from separate calculations of those parts of the molecule whose interactions ought to be analyzed, can be divided into occupied and unoccupied orbitals. In case of correlated wave functions the natural molecular

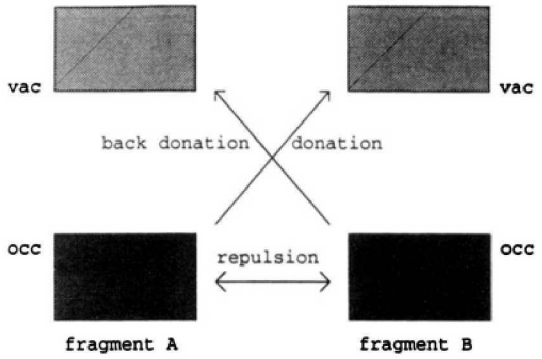

Figure 1. Schematic representation of the three components of the LCFO wave function.

orbitals (NMO) φ_i^{nat} of the complex are expressed as a linear combination of the canonical molecular orbitals (CMO) Φ_μ of the fragments. The charge donation d_i from fragment A to fragment B can then be defined as

$$d_i = \sum_k^{occ,A} \sum_n^{vac,B} m_i c_{ki} c_{ni} \langle \Phi_k | \Phi_n \rangle \tag{7}$$

for every orbital of the molecule. Summation of d_i leads to the overall charge donation from A to B. In a similar manner, back donation b_i can be written as

$$b_i = \sum_l^{occ,B} \sum_m^{vac,A} m_i c_{li} c_{mi} \langle \Phi_l | \Phi_m \rangle \tag{8}$$

The closed-shell interaction of the two fragments is then defined by

$$r_i = \sum_k^{occ,A} \sum_m^{occ,B} m_i c_{ki} c_{mi} \langle \Phi_k | \Phi_m \rangle \tag{9}$$

While the donation and back donation terms d_i and b_i can easily be interpreted as charge donation between the fragments, the closed-shell interaction term r_i is more difficult to understand. Since the r_i terms are calculated from the overlap of the occupied orbitals of the fragments, a positive sign would indicate an accumulation of charge in this region. A negative sign would mean that electronic charge is removed from the occupied/occupied region of the fragment orbitals. As will be shown below, the sum of the r_i terms are always negative. This is reasonable, because the interactions between filled orbitals are repulsive. A plausible interpretation of the r_i terms is that they indicate the change in the repulsive polarization, i.e., the r_i term gives the amount of electronic charge which is removed from the overlap of the occupied MOs into the nonoverlapping regions. Therefore, we call this term charge polarization.

It should be mentioned that polarization effects and exchange repulsion are included in this scheme. Therefore it is possible to characterize every MO in a molecule concerning its role in the charge reorganization. Figure 1 shows schematically the three components of the LCFO wave function.

It is possible to calculate the LCFO wave function of AB from the fragment orbitals of A and B using geometries for A and B which are taken from the optimized geometry of AB and kept frozen, or it is possible to use the optimized geometries of the separate fragments. The latter approach has been used to study the change in the electronic structure of A and B along a reaction coordinate,[18] i.e. the MOs of AB at the transition state have been expressed as linear combination of the MOs of the educt A + B.[18a] The problem with this approach is that the LCFO wave function is not invariant to the choice of the coordinate system. At present we are using the geometries of the fragments A and B from the optimization of AB. The LCFO wave function is then constructed from the direct sum of the orbitals of A and B, which have been calculated with the same coordinates as in AB. This avoids possible changes in the MOs which might be caused by coordinate transformation.

The calculation of the charge decomposition terms as described above will be subject to the basis set superposition error (BSSE),[22] because the basis set of each fragment is augmented by the unoccupied orbitals of the other fragment. Thus, part of the charge donation is caused not by donor–acceptor interactions but rather by the augmentation of the basis sets. To estimate the effect of the basis set augmentation upon the CDA results, we calculated the donation, back donation, and charge polarization terms using two different basis sets, i.e., 6-31G(d)[23] and TZ2P.[24] In case of H_3BCO and H_3BNH_3 we give additional results at the HF/3-21G[25] and HF/6-311G-(d,p)[26] levels of theory. It should be emphasized at the outset that the absolute values of the calculated CDA terms have no physical meaning. It is the relative magnitude of the different terms, in particular the donation and back donation terms, which is important for the development of chemical models based on quantum mechanics.

To actually carry out the charge decomposition analysis, the following steps are recommended:

1. Calculate the MOs of the complex in its equilibrium structure.
2. Calculate the MOs of fragment A and B using the coordinates of the complex.
3. Combine the MOs of the two fragments, i.e., calculate the direct sum.
4. Calculate the eigenvectors of the complex in the basis of the fragment MOs.
5. Calculate the overlap integrals in the basis of the fragment MOs (similarity transformation).
6. Calculate the terms d_i, b_i, and r_i by the sum of the respective orbital contributions given by eqs 7–9.

Steps 1 and 2 can be accomplished by every standard quantum mechanical package. Steps 3–6 can be carried out by a C program available from the authors,[27] which is written to read output files from a Gaussian92[28] calculation but can in principal be used in combination with any other quantum mechanical program.

The quantum mechanical calculations of this study have been carried out using the program package Gaussian92.[28] Geometry optimizations were performed at the HF/6-31G(d) and MP2/6-31G(d) levels of theory. The quasi-relativistic ECPs developed by Hay and Wadt[29] were used for the transition metals with a split valence basis set [441/2111/21] for W, [441/2111/31] for Ag, and [441/2111/21] for Au. The ECPs for W, Ag, and Au incorporate the mass velocity and Darwin relativistic terms into the potential.[29] The CDA was carried out at the same levels of theory. In addition, the CDA terms have been calculated using the TZ2P basis set for the first and second row elements in conjunction with a [4311/2111/*N*11/11] ($N = 1$ for W and Au, $N = 2$ for Ag) ECP valence basis set for the metals.[29] The exponents for the f-type polarization functions[30] are 1.646 and 0.412 for W, 3.222 and 0.806 for Ag, and 2.100 and 0.525 for Au.

Results and Discussion

We first examine the donor–acceptor complexes H_3BCO and H_3BNH_3. Both are strongly bound complexes, which have been extensively investigated computationally[31] with several inter-

TABLE 1: Calculated and Experimental Equilibrium Geometries for H_3BCO and H_3BNH_3 (Distances in Å, Angles in deg)

	r(BH)	a(HBH)	r(CO) r(NH)	a(HNH)	r(BC) r(BN)	D_e	D_0
			H_3BCO (C_{3v})				
HF/6-31G(d)	1.203	115.1	1.108		1.627	9.2	5.8
MP2/6-31G(d)	1.206	114.3	1.149		1.551	25.6	22.2
exp[a]	1.221	114.5	1.135		1.534		24.6
			H_3BNH_3 (C_{3v})				
HF/6-31G(d)	1.209	114.1	1.004	108.0	1.689	23.4	18.0
MP2/6-31G(d)	1.210	113.9	1.020	107.8	1.664	34.6	29.2
exp[b]	1.216	113.8	1.014	108.7	1.657		31.1

[a] Reference 45. [b] Reference 46.

pretation schemes employed. Earlier work in the field of donor−acceptor (DA) complexes predicated that the stabilization was primarily due to the charge-transfer interactions.[32] Later Hanna et al.[33] suggested that electrostatic attractions are the source of the principal bonding interactions. However, Mulliken and Person[34] proposed that electrostatic forces are likely to dominate bonding only in weak DA complexes.

More recent, quantum chemical calculations provided insight into this problem. In the work of Morokuma,[35] H_3BCO is called a "CT-PL-ES" complex, which means that charge transfer as well as polarization effects and electrostatic interactions are responsible for the attraction of the fragments. A breakdown of the energy contributions of donation and back donation was also given in this work. The relative importance was estimated as (donation/back donation) ~ (2/1). In H_3BNH_3, the electrostatic interaction is suggested as the dominant attractive component with charge transfer and polarization playing a less significant role. In contrast to this, Roeggen[31a] adopted an interpretation scheme which stresses the role of charge transfer for stabilization in both molecules. A very recent theoretical study[36] using the NBO partitioning scheme and the topological analysis of the electron density distribution comes to the conclusion that the bonding in the strongly bound donor−acceptor complexes of BH_3, BF_3, and BCl_3 have large covalent contributions, while the bonds in the more weakly bound complexes are dominated by electrostatic interactions.[36] However, the study also shows that electrostatic interactions are dominant in the strongly bound complex Cl_3AlNMe_3, while the related complex Cl_3BNMe_3 is mainly bound by charge-transfer (covalent) interactions.

As a starting point for the bonding analysis we carried out geometry optimizations at the HF/6-31G(d) and MP2/6-31G(d) levels of theory. Table 1 shows the calculated and experimental bond lengths of H_3BCO and H_3BNH_3. For both complexes a C_{3v} geometry is predicted. The structures were confirmed to be energy minima by frequency calculations. In H_3BNH_3 the staggered conformation, similar to the isoelectronic ethane, yields the lowest energy, in accordance with experiment.[37]

The optimized geometries at MP2/6-31G(d) of H_3BNH_3 and H_3BCO are in good agreement with experiment (Table 1). The HF/6-31G(d) optimized geometry of H_3BNH_3 has a slightly longer B−N bond, while the B−C bond of H_3BCO is nearly 0.1 Å longer than experimentally observed. It has been shown that the donor−acceptor bond lengths of strongly bound complexes are calculated in reasonable agreement with experiment at the HF level, while weaker bound complexes are predicted with bond lengths which are too long.[36] Table 1 shows also the calculated and experimental dissociation energies. It is obvious that H_3BNH_3 is stronger bound than H_3BCO.

Table 2 shows the results of the charge decomposition analysis for H_3BCO at the optimized geometry calculated at HF/6-31G(d) and MP2/6-31G(d). *d* denotes the charge transfer from CO to BH_3, whereas *b* indicates the amount of back donation. The electron repulsion term *r* is listed in the fourth column. We discuss the HF/6-31G(d) results first.

TABLE 2: Charge Components of the Canonical (Natural) Orbitals of H_3BCO at the HF(MP2) Level[a]

orb	occ	*d*	*b*	*r*
$1a_1$	2.0(2.00)	0.000(+0.001)	0.000(0.000)	0.000(0.000)
$2a_1$	2.0(2.00)	+0.002(0.000)	0.000(+0.001)	0.000(0.000)
$3a_1$	2.0(2.00)	0.000(0.000)	−0.001(0.000)	0.000(0.000)
$4a_1$	2.0(1.99)	−0.026(+0.016)	−0.001(−0.001)	−0.006(+0.065)
$5a_1$	2.0(1.98)	+0.083(−0.013)	−0.007(−0.032)	+0.232(+0.251)
$6a_1$	2.0(1.96)	+0.075(+0.324)	−0.040(+0.045)	+0.213(−0.166)
$1e_1$	2.0(1.95)	−0.001(−0.004)	+0.001(−0.003)	+0.022(−0.053)
$1e_1$	2.0(1.95)	−0.001(−0.004)	+0.001(−0.003)	+0.022(−0.053)
$7a_1$	2.0(1.97)	0.343(+0.245)	+0.054(+0.013)	−0.741(−0.369)
$2e_1$	2.0(1.97)	−0.001(+0.001)	+0.087(+0.123)	−0.029(+0.029)
$2e_1$	2.0(1.97)	−0.001(+0.001)	+0.087(+0.123)	−0.039(+0.029)
Σa_1		+0.477(+0.563)	+0.006(+0.013)	−0.301(−0.224)
Σe_1		−0.005(−0.013)	+0.176(+0.240)	−0.034(−0.048)
Σ		+0.472(+0.550)	+0.182(+0.253)	−0.335(−0.272)
Σ	HF//MP2	+0.521	+0.220	−0.354
Σ	TZ2P	+0.485(+0.499)	+0.172(+0.228)	−0.405(−0.412)

[a] Note that there is no one-to-one correlation between a CMO and an NMO; see text.

The calculated charges d_i, b_i, and r_j computed for each orbital characterize its role in the bond formation. The three lowest lying orbitals are the 1s orbitals of O, C, and B, respectively. These orbitals show nearly no change, emphasizing the fact that core orbitals do not play any role in the bonding interactions. As expected, the three highest lying orbitals are strongly involved in the bonding mechanism. The $7a_1$ orbital represents the σ donation from the carbon lone pair MO of CO to BH_3, which is considered as the primary source for the donor−acceptor bonding. The $7a_1$ orbital has 0.343 electron, which is donated from CO to BH_3. There is also a small back donation of 0.054 e from BH_3 to CO in the $7a_1$ orbital. The highest lying degenerate $2e_1$ orbital has π symmetry. There are 0.174 electrons shifted in this orbital, which has π-back-donating character, from BH_3 to CO. There are also small negative contributions by the donating/back-donating components. These contributions occur because of polarization effects which are also included in *d* and *b*. Inspection of the repulsion terms reveals that the four-electron repulsive interactions are diminished (negative sign) in the $7a_1$ and $2e_1$ orbitals. A very large contribution is calculated for the $7a_1$ orbital (−0.741 e). This means that 0.741 electron is removed from the overlapping area of the occupied/occupied MOs of BH_3 and CO in H_3BCO.

The results in Table 2 also show that lower lying valence orbitals are involved in the bonding mechanism: The MOs $5a_1$ and $6a_1$ show significant σ-charge donation from CO to BH_3. However, the repulsive character of the $5a_1$ and $6a_1$ orbitals is reflected in the significant repulsion term *r* (+0.232 e and +0.213 e). Figure 2 shows contour plots of the $5a_1$, $6a_1$, $7a_1$, and $2e_1$ canonical orbitals of H_3BCO.

The summation over all occupied orbitals gives the total amount of charge reorganization. 0.472 electron is shifted from CO into the bonding region, while 0.182 electron is back donated from BH_3. The reduced closed-shell repulsion in comparison with the superimposed fragments is demonstrated by the negative sign of *r* (−0.335 electron). Table 2 shows that the OC → BH_3 donation and the repulsive polarization are largely due to orbitals having a_1 symmetry, while the H_3B → CO back donation is mainly caused by e_1 orbitals.

Now we investigate the charge partitioning of H_3BCO calculated at the MP2/6-31G(d) level of theory. Table 2 shows

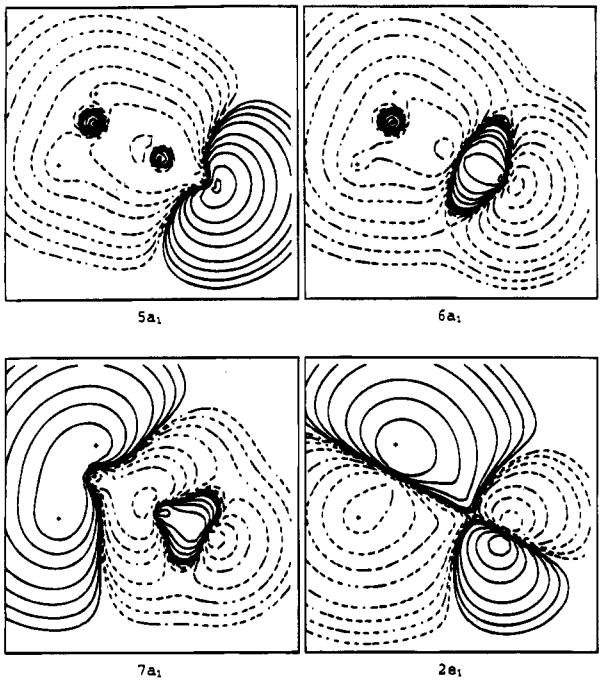

Figure 2. Plots of the $5a_1$, $6a_1$, $7a_1$, and $2e_1$ canonical orbitals of H_3BCO at HF/6-31G(d)//HF/6-31G(d).

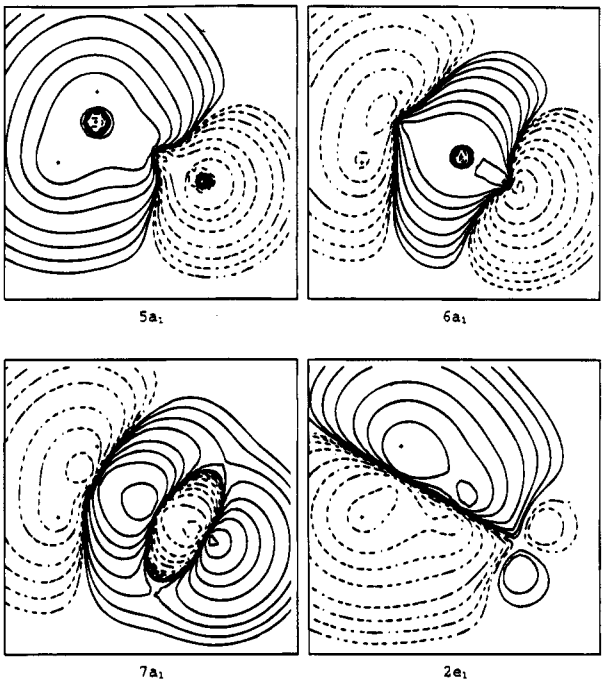

Figure 3. Plots of the $5a_1$, $6a_1$, $7a_1$, and $2e_1$ natural orbitals of H_3BCO at MP2/6-31G(d)//MP2/6-31G(d).

the donating, back-donating, and repulsive contributions to the natural orbitals with an occupation number >1.0. There are significant differences compared to the results calculated at the HF level. The donating contributions from CO to BH_3 are larger at MP2/6-31G(d). There are *two* natural orbitals, which dominate the donation from CO to BH_3, the $6a_1$ and $7a_1$ MO. It is important for a comparison of the results at the HF and MP2 level of theory to realize that there is no direct correlation between a canonical and a natural orbital. Natural orbitals do not have energy eigenvalues. The NMOs listed in Table 2 are ordered by symmetry and then by occupancies. This means that the NMOs have the same symmetry as the CMOs, but a NMO of a given symmetry does not correspond to a particular CMOs. Therefore, the ordering of the NMOs within a given symmetry is somewhat arbitrary. Figure 3 shows the plots of the $5a_1$, $6a_1$, and $7a_1$ NMOs. The shape of the natural orbitals shows a strong mixing of the canonical orbitals of the same symmetry.

Back donation is larger at the MP2/6-31G(d) level, because the $2e_1$ MOs donate 0.123 e each. Figure 3 shows that the $2e_1$ natural orbital has a larger extension at the carbon end and a smaller coefficient at oxygen than the $2e_1$ canonical orbital (Figure 2). The overall effect of correlation is to produce an increase of the electron donation from 0.472 e to 0.550 e, an increase of the back donation from 0.182 e to 0.253 e and a reduction of the repulsive interactions from −0.335 e to −0.272 e. This gives a total of 1.075 electrons which are rearranged due to bond formation. At the HF/6-31G(d) level only 0.989 electron is rearranged. Part of the difference between the values at HF/6-31G(d) and MP2/6-31G(d) is because of the different geometries. Table 2 also shows the amount of donation/back donation at the HF/6-31G(d) level using the MP2/6-31G(d) optimized geometries.

A significant amount of electronic charge is removed from the overlapping area of the occupied/occupied orbitals. Table 2 shows that the a_1 orbitals dominate the repulsive polarization. At the HF level, the a_1 CMOs contribute −0.301 electrons from the total amount of −0.335 electrons. The individual contributions of the a_1 NMOs to the repulsive polarization are different in magnitude and even in the sign from the a_1 CMOs (Table 2). The total contribution of the a_1 NMOs is similar (−0.224 electron), however, to the a_1 CMOs. The same holds true for the *r* contributions of the e_1 orbitals.

In agreement with previous work[31,36] the charge decomposition analysis shows that there is a considerable amount of charge transfer from both fragments into the bonding region. This emphasizes the important role of nonelectrostatic contributions. The ratio of donation/back donation (ca. 2/1) is in agreement with the estimate of the relative energetic contributions by Morokuma.[35]

The differences between the total *d* and *b* contributions may be used to estimate the partial charges on the fragments. The results in Table 2 show that 0.550 electron is donated from CO to BH_3 to 0.253 electron is back donated from BH_3 to CO. This gives at MP2/6-31G(d) a positive partial charge of 0.297 electron at CO in H_3BCO. The NBO analysis at the MP2/6-31G(d) level gives a partial charge of +0.44 e at CO in H_3BCO.[36]

Table 2 also shows the calculated total *d*, *b*, and *r* contributions using the TZ2P basis set. The extent of the donation and back donation at the HF/TZ2P level is very similar to that at HF/6-31G(d). Both terms are ca. 10% smaller at MP2/TZ2P than at MP2/6-31G(d). The charge polarization term *r* becomes larger using the larger basis set. An important result is that the ratio of donation to back donation changes very little when a larger basis set is employed. The donation and repulsive polarization at the correlated level is mainly caused by a_1 orbitals and the back donation is caused by e_1 orbitals.

The charge decomposition analysis for the borazane molecule calculated at HF/6-31G(d) and MP2/6-31G(d) is shown in Table 3. The similarities and differences with respect to H_3BCO are obvious. The core orbitals remain nearly unchanged. Large contributions to the donor−acceptor interactions are calculated for the $4a_1$ and $5a_1$ MOs, which are shown in Figure 4. The charge donation from NH_3 to BH_3 is mainly due to the $5a_1$ MO (0.283 e). Table 3 shows that there is practically no back donation from BH_3 to NH_3. There is a large depletion of electronic charge in the overlapping region of the occupied orbitals of BH_3 and NH_3, which form the $5a_1$ MO (−0.643 e).

TABLE 3: Charge Components of the Canonical (Natural) Orbitals of H_3BNH_3 at the HF(MP2) Level

orb	occ	*d*	*b*	*r*
$1a_1$	2.0(2.00)	0.000(0.000)	0.000(0.000)	0.000(0.000)
$2a_1$	2.0(2.00)	0.000(0.000)	0.000(0.000)	0.000(0.000)
$3a_1$	2.0(1.99)	+0.042(−0.009)	−0.001(−0.016)	+0.031(+0.290)
$1e_1$	2.0(1.98)	−0.013(+0.001)	0.000(+0.005)	+0.033(+0.022)
$1e_1$	2.0(1.98)	−0.013(+0.001)	0.000(+0.005)	+0.033(+0.022)
$4a_1$	2.0(1.98)	+0.059(+0.070)	−0.022(−0.002)	+0.342(−0.267)
$5a_1$	2.0(1.96)	+0.283(+0.367)	+0.002(+0.013)	−0.643(−0.269)
$2e_1$	2.0(1.97)	−0.002(−0.015)	+0.001(0.000)	−0.088(−0.081)
$2e_1$	2.0(1.97)	−0.002(−0.015)	+0.001(0.000)	−0.088(−0.081)
Σa_1		+0.384(+0.418)	−0.020(−0.008)	−0.270(−0.249)
Σe_1		−0.030(−0.036)	+0.003(+0.008)	−0.108(−0.118)
Σ		+0.354(+0.382)	−0.017(0.000)	−0.378(−0.367)
Σ	HF//MP2	+0.367	−0.017	−0.397
Σ	TZ2P	+0.394(+0.362)	−0.014(−0.006)	−0.368(−0.385)

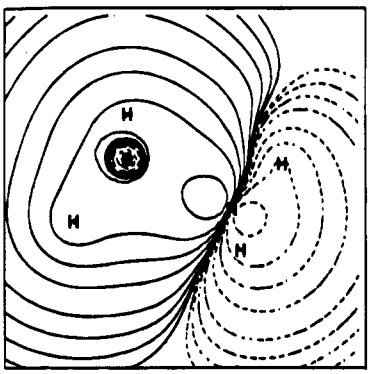

$4a_1$

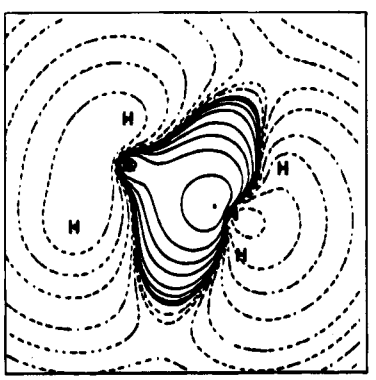

$5a_1$

Figure 4. Plots of the $4a_1$ and $5a_1$ canonical orbitals of H_3BNH_3 at HF/6-31G(d)//HF/6-31G(d).

The $4a_1$ orbital shows an accumulation of electronic charge of 0.342 e in the occupied/occupied overlap region of the fragments.

Table 3 also shows that the sum of the donating, back-donating, and repulsive contributions change very little when going from the HF/6-31G(d) level to MP2/6-31G(d). The back donation is exactly zero, and the donation from NH_3 to BH_3 is calculated to be 0.382 electron. This means that the BH_3 group of H_3BNH_3 is predicted to carry a partial negative charge of −0.382 electron, which is more than the partial charge in H_3BCO (0.297 e). This is reasonable because NH_3 is a better donor than CO. However, we want to point out that the total amount of electronic charge which is donated from the donor and the acceptor into the bonding region is larger for H_3BCO (0.803 e, Table 2) than for H_3BNH_3 (0.382 e, Table 3). This conclusion is in agreement with results from a topological analysis of the electronic structure of H_3BCO and H_3BNH_3.

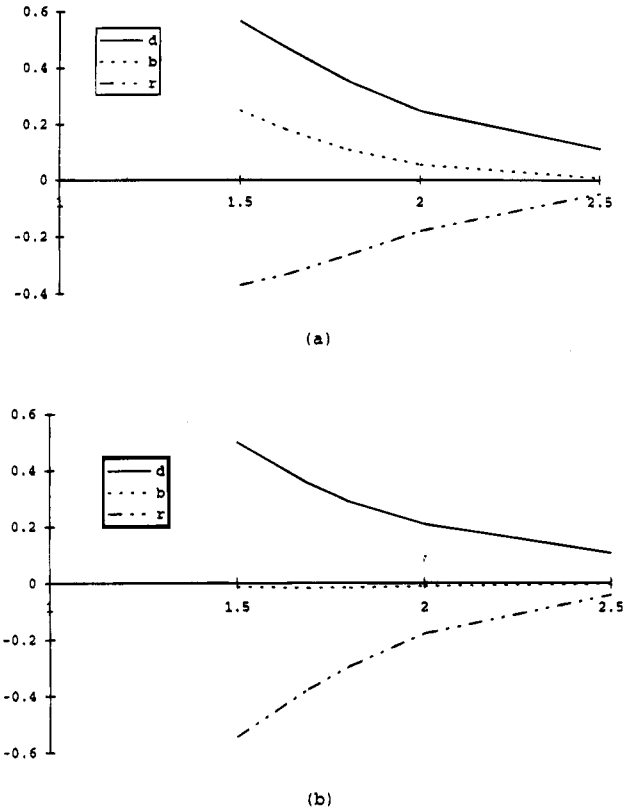

Figure 5. Charge donation, back donation, and repulsion of H_3BCO (a) and H_3BNH_3 (b) at different B−C and B−N distances. The remaining geometric variables were held fixed at the optimized HF/6-31G(d) geometry.

These results indicate that the donor−acceptor bond of the former complex has a higher covalent character than the latter.[36] H_3BNH_3 is more strongly bound than H_3BCO because the Coulomb interactions are stronger in H_3BNH_3 than in H_3BCO.

Table 3 shows that the results of the CDA carried out at the HF and MP2 levels of theory using the TZ2P basis set are very similar to those calculated using the 6-31G(d) basis set. The results of the CDA method suggests that π back donation from BH_3 to NH_3 is negligible, while the back donation of BH_3 to CO is significant. A similar result concerning the π-acceptor abilities of CO and NH_3 has been reported in a study of copper complexes Cu_nCO and Cu_nNH_3 (n = 1, 5) using the CSOV technique.[15c]

Distance Dependency and Basis Set Dependency of the Charge Components

To investigate bond formation along a reaction coordinate, we calculated the magnitude of the charge component terms at different boron−carbon and boron−nitrogen distances. The results are shown in Figure 5.

As expected, the sum of the charge terms $\Sigma(d)$, $\Sigma(b)$, and $\Sigma(r)$ approach zero at large distances. The onset of the donating contribution is much earlier than the back donation, because the former interaction arises mainly by the σ orbitals, while the back donation has largely π character. Figure 5 demonstrates clearly that the largest difference between the two complexes is in the size of the back donation from the acceptor to the donor, which is negligible for H_3BNH_3.

To estimate the basis set dependency of the CDA method, we calculated the charge components of the two complexes using four different basis sets, i.e., 3-21G, 6-31G(d), 6-311G-(d,p), and TZ2P at the HF/6-31G(d) optimized geometries. There are large changes of the d and b contributions using the 3-21G

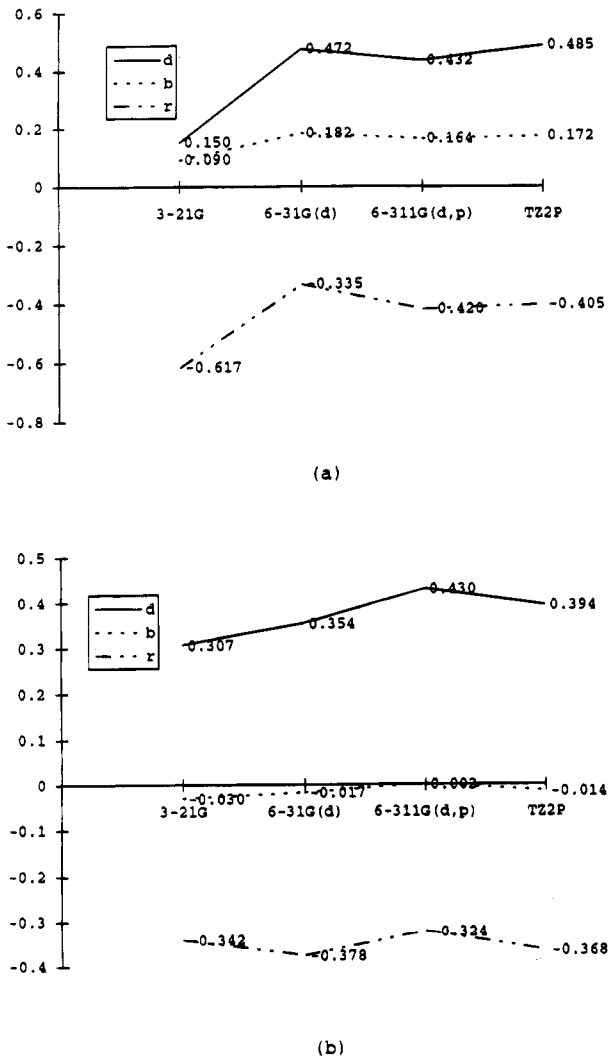

Figure 6. Basis set dependency of canonical orbital charge components of H_3BCO (a) and H_3BNH_3 (b) at the HF/6-31G(d) optimized geometries.

and 6-31G(d) basis sets for H_3BCO (Figure 6a). The relative size of the three contributions remain fairly constant for the two complexes using the 6-31G(d), 6-31G(d,p), and TZ2P basis sets. It is obvious that the analysis of the wave function using the CDA partitioning scheme should be carried out using at least a 6-31G(d) basis set.

Transition-Metal Carbonyls

The classical model to describe the electronic structure of transition metal complexes in terms of molecular orbitals has been given by Dewar, Chatt, and Duncanson (DCD).[13] The DCD model describes metal−ligand bonding in terms of electron donation from occupied ligand orbitals to empty (s, p, or d type) orbitals of the metal and back donation from occupied metal d orbitals to empty ligand orbitals. Because the former orbitals have usually σ symmetry, while the latter have π symmetry, the metal−ligand bond is described in terms of σ-donation/π-back donation. Typical examples for which the DCD model has been frequently used are the transition metal carbonyl complexes. There has been much discussion about the relative strength of the donating/back donating components of the metal−ligand interactions in this class of compounds.[16,38]

The charge decomposition analysis is ideally suited to analyze the metal−ligand bonding in terms of orbital interactions, which may in the particular case of transition-metal complexes be considered as a quantitative expression of the DCD model. We have chosen two extreme examples of transition-metal carbonyl complexes to demonstrate the performance of the model. One example is tungsten hexacarbonyl $W(CO)_6$. $W(CO)_6$ is a "classical" carbonyl complex, i.e., the C−O stretching frequency of the complex is *lower* (2117 cm^{-1})[39] than in isolated CO (2143 cm^{-1}).[40] The lower C−O stretching frequency is usually interpreted as the result of d(M) → π *(CO) back donation, which weakens the CO bond. There is another class of transition-metal carbonyl complexes, which is termed "nonclassical" because the C−O stretching mode is shifted towards *higher* wavenumbers relative to free CO.[41a] A growing number of examples has been reported in recent years for this class of compounds.[41−43] Two cases are $Ag(CO)^+$ and $Au(CO)^+$. The C−O stretching frequencies of salt compounds of $Ag(CO)^+$ are ca. 60 cm^{-1} higher than in CO. The experimentally observed C−O stretching mode of Au(CO)X (X = halogen) compounds is 11−53 cm^{-1} higher than in CO.[43] The unusual increase of the C−O stretching mode in these and other metal complexes has been interpreted as the result of negligible π-back donation.[42−44]

TABLE 4: Calculated and Experimental Bond Lengths (Å) of $W(CO)_6$ and MCO^+ (M = Ag, Au)

		r(M−C)	r(C−O)
$W(CO)_6$	HF	2.106	1.122
	MP2	2.060	1.166
	exp[a]	2.058	1.148
$AgCO^+$	HF	2.511	1.103
	MP2	2.329	1.143
	exp[b]	2.100	1.077
$AuCO^+$	HF	2.145	1.099
	MP2	1.975	1.143
	exp[c]	1.932	1.113

[a] Reference 47. [b] Reference 43. [c] Reference 48.

We begin the discussion with $W(CO)_6$. Table 4 shows the calculated and experimental bond lengths. The theoretically predicted W−C bond length at the MP2 level of theory is in excellent agreement with the experimental value, while the HF distance is slightly too long. The calculated C−O interatomic distances at HF and MP2 are slightly too short and too long, respectively.

The calculated donating and back-donating contributions by the fragment orbitals of $W(CO)_6$ are shown in Table 5. It is illuminating to discuss the results in comparison with a qualitative orbital interaction diagram between a central atom M and an octahedral ligand fragment L_6 shown in Figure 7.

Figure 7a shows for didactical purposes only the interactions between the σ-donating orbitals of the ligands and the central atom. The six carbon lone-pair orbitals of the CO ligands form a set of e_g, t_{1u}, and a_{1g} orbitals, which may donate electrons into the formally empty e_g(d), a_{1g}(s), and t_{1u}(p) AOs of the tungsten atom. Table 5 shows that the calculated donations arise exactly from these orbital interactions. The largest contribution is calculated for the σ donation from the t_{1u} lone-pair orbital of CO into the t_{1u}(p) AO of W. The donation is 0.169 e at the HF level and 0.166 e at the MP2 level. Note that only one component of the triply degenerate t_{1u} canonical orbital has a donating contribution, because the charge decomposition analysis is carried out for the interaction between *one* CO and $W(CO)_5$. The t_{1u} natural orbitals are accidentally rotated. Therefore, the interactions between CO and $W(CO)_5$ show contributions by all three components of the t_{1u} orbital. Note also that the natural orbitals are ordered by comparing their symmetry and shape with that of the canonical orbitals.

The donation from the e_g lone-pair orbital of CO into the e_g(d) AO of W is slightly less than the t_{1u} MO, 0.143 e at the HF level, and 0.150 e at the MP2 level. The donation from the a_{1g} lone-pair orbital of CO into the a_{1g}(s) AO of W is much

TABLE 5: Charge Components for the Canonical (Natural) MOs of $W(CO)_6$ at the HF(MP2) Level

orb	occ	*d*	*b*	*r*
a_{1g}	2.0(1.96)	+0.010(−0.002)	−0.001(−0.003)	+0.068(+0.007)
e_g	2.0(1.97)	0.000(−0.001)	−0.004(−0.001)	−0.028(−0.008)
e_g	2.0(1.97)	0.000(−0.003)	0.000(−0.004)	0.000(−0.022)
t_{1u}	2.0(1.95)	0.000(+0.001)	+0.001(+0.004)	+0.001(+0.010)
t_{1u}	2.0(1.95)	0.000(+0.003)	+0.001(+0.021)	+0.001(−0.046)
t_{1u}	2.0(1.95)	−0.002(+0.004)	−0.003(+0.025)	−0.020(+0.056)
a_{1g}	2.0(1.98)	+0.024(+0.036)	−0.008(−0.005)	+0.066(+0.097)
t_{2g}	2.0(1.95)	0.000(+0.013)	0.000(−0.004)	0.000(−0.071)
t_{2g}	2.0(1.95)	+0.003(+0.007)	+0.003(−0.002)	+0.029(−0.033)
t_{2g}	2.0(1.95)	+0.003(+0.005)	+0.003(−0.002)	+0.029(−0.018)
t_{1u}	2.0(1.97)	+0.023(+0.003)	−0.003(+0.002)	+0.011(−0.005)
t_{1u}	2.0(1.97)	+0.003(+0.013)	+0.001(−0.002)	+0.023(−0.034)
t_{1u}	2.0(1.97)	+0.003(+0.011)	+0.001(−0.001)	+0.023(−0.029)
e_g	2.0(1.96)	0.000(+0.048)	0.000(+0.008)	0.000(−0.018)
e_g	2.0(1.96)	+0.143(+0.102)	+0.015(+0.016)	−0.079(−0.037)
t_{2u}	2.0(1.95)	0.000(+0.001)	0.000(−0.002)	0.000(−0.006)
t_{2u}	2.0(1.95)	0.000(+0.001)	0.000(−0.002)	−0.004(−0.006)
t_{2u}	2.0(1.95)	0.000(0.000)	0.000(0.000)	−0.004(0.000)
t_{1g}	2.0(1.95)	0.000(0.000)	0.000(0.000)	0.000(−0.003)
t_{1g}	2.0(1.95)	+0.002(+0.001)	0.000(−0.003)	−0.015(−0.018)
t_{1g}	2.0(1.95)	+0.002(+0.001)	0.000(−0.002)	−0.015(−0.017)
t_{1u}	2.0(1.96)	0.000(+0.130)	+0.004(−0.003)	−0.020(−0.113)
t_{1u}	2.0(1.96)	0.000(+0.015)	+0.004(+0.004)	−0.020(+0.001)
t_{1u}	2.0(1.96)	+0.169(+0.021)	−0.014(+0.004)	−0.226(−0.005)
t_{2g}	2.0(1.91)	0.000(−0.003)	0.000(+0.050)	0.000(−0.034)
t_{2g}	2.0(1.91)	−0.008(−0.006)	+0.093(+0.086)	−0.048(−0.058)
t_{2g}	2.0(1.91)	−0.008(−0.005)	+0.093(+0.073)	−0.048(−0.050)
Σa_{1g}		+0.033(+0.023)	−0.011(−0.008)	+0.138(+0.145)
Σe_g		+0.133(+0.111)	+0.009(+0.015)	−0.105(−0.071)
Σt_{1u}		+0.195(+0.166)	−0.009(+0.044)	−0.224(−0.139)
Σt_{2g}		−0.010(+0.011)	+0.188(+0.191)	−0.037(−0.184)
Σt_{2u}		0.000(+0.002)	0.000(−0.004)	−0.007(−0.007)
Σt_{1g}		+0.003(+0.002)	0.000(−0.005)	−0.027(−0.022)
Σ		+0.354(+0.315)	+0.177(+0.233)	−0.262(−0.278)
Σ	HF//MP2	+0.342	+0.177	−0.307
Σ	TZ2P	+0.376(+0.316)	+0.156(+0.184)	−0.274(−0.305)

less, only 0.024 e at HF and 0.036 e at MP2 (Table 5). The calculated total donation from CO to W is 0.354 e at HF and 0.315 e at MP2. Figure 8 shows the contour line diagrams of the most important σ-donating orbitals of $W(CO)_6$.

We now discuss the back donation from W to CO. Figure 7b shows that the major contribution can be expected from the occupied t_{2g}(d) AOs of W donating into the π^* CO orbitals. Because CO has a degenerate set of π^* MOs, two contributions arise for each CO ligand. The calculated charge donation from the charge decomposition analysis shows (Table 5) that the only significant back donation arises from the t_{2g}(d) AOs at W into the π^*(CO) orbitals. The calculated back donation is 0.186 e at HF and 0.159 at MP2. The total amount of back donation from W to CO is 0.177 e at HF and 0.233 e at MP2. Thus, the magnitude of the metal-to-ligand donation becomes smaller and the back donation becomes larger at the correlated level. This is mainly due to correlation effects and not to the different equilibrium geometries at the HF and MP2 levels. Table 5 shows that the donation and back donation contributions at the HF level using the MP2 geometry are similar to the HF//HF values. The calculated donation OC → W becomes slightly larger and the W → CO back donation becomes slightly smaller at HF/TZ2P than at HF/6-31G(d) (Table 5). The values at HF/TZ2P and at MP2/TZ2P indicate that the results using the two basis sets are very similar.

The charge decomposition analysis shows also that there is a significant charge reorganization at the fragments. The occupied/occupied repulsion term indicates that 0.262 electrons (0.278 e at the HF level) are removed from the overlap region. The breakdown of the donation, back donation, and charge polarization terms into orbital contributions of different symmetry shows that the OC → W donation is mainly due to the t_{1u} and e_g orbitals, while the W → CO back donation is mainly caused by the t_{2g} orbitals (Table 5). The repulsive polarization at the HF level is mainly caused by t_{1u}, a_{1g} and e_g orbitals, while at the MP2 level the t_{2g}, a_{1g}, t_{1u}, and to a less extent the e_g orbitals are important.

The charge decomposition analysis at the HF and correlated levels gives a larger contribution for the CO → W donation (0.315 e at MP2) than for the W → CO back donation (0.233 e at MP2). This means that the calculated partial charges of

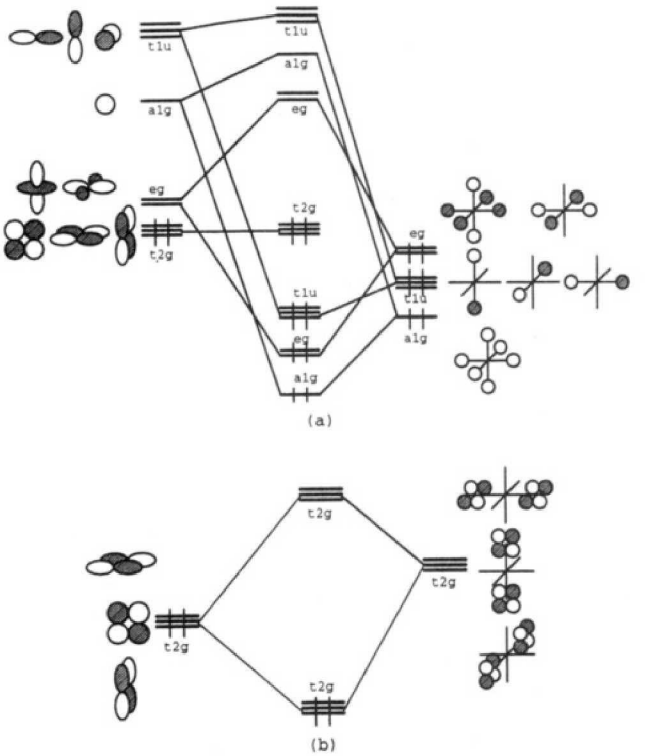

Figure 7. Development of the molecular orbitals of an octahedral ML_6 complex, where L is a σ-donor ligand (a) and schematical representation of the interactions of the t_{2g} d orbitals of a metal with the appropriate symmetry-adapted π^* orbitals of the ligands (b).

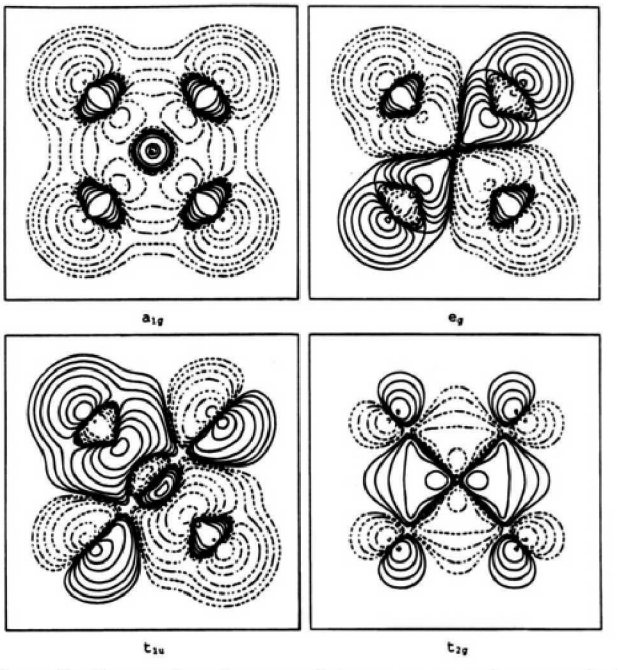

Figure 8. Contour line diagrams of the a_{1g}, e_g, t_{1u}, and t_{2g} canonical orbitals of $W(CO)_6$ at the HF/(441/2111/21)/6-31G(d) level.

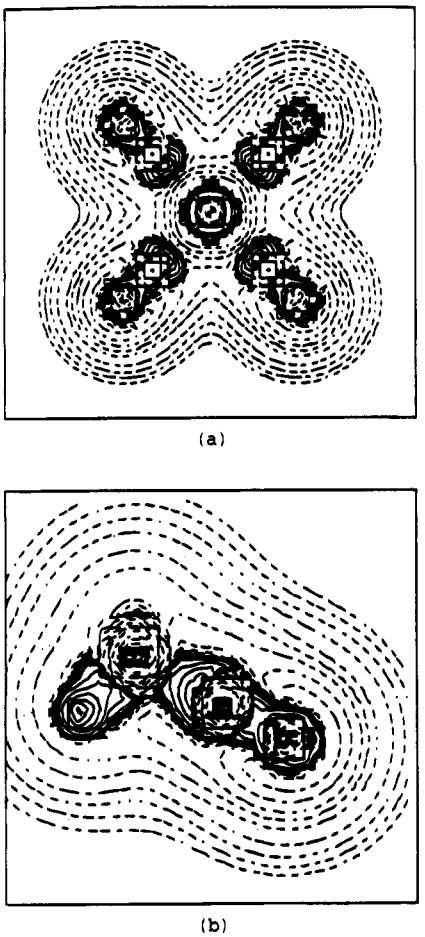

Figure 9. Laplacian distribution of $W(CO)_6$ and H_3BCO at the MP2 level of theory.

$W(CO)_6$ at the MP2 level are $q(CO) = +0.082$ and $q(W) = -0.492$. The slightly larger OC → W donation than W → CO back donation calculated at MP2/6-31G(d) should *not* be considered as evidence that the ligand-to-metal donation is stronger than the back donation. The relative magnitude of the two contributions has been discussed controversely in the past.[38] The CDA results suggest that in $W(CO)_6$ both contributions have the same order of magnitude. The real value of the CDA method lies in the possibility of comparing quantitatively the *relative* contributions of different ligands, as shown above for H_3BCO and H_3NH_3. Theoretical studies of complexes $M(CO)_nL$ for different metals M and ligands L using the CDA method are underway.

A comparison of the charge decomposition analysis of $W(CO)_6$ and H_3BCO is very informative. We compare only the MP2 values. The total amount of electronic charge, which is donated from the fragments into the W−CO overlapping region (donation plus back donation) is 0.548 e. The population of the bonding region of H_3BCO by the donation and back donation is 0.803 e, which is significantly larger than for $W(CO)_6$. The partial charge at CO is also larger in H_3BCO (+0.297) than in $W(CO)_6$ (+0.082), which indicates less electronic interactions for the carbonyl bonds of $W(CO)_6$ than for H_3BCO. This is in good agreement with the Laplacian distribution[11] of the total electronic charge of the X−CO bonding region of the two compounds shown in Figure 9. It is obvious that the deformation of the charge distribution at CO caused by the bond formation is much stronger in H_3BCO than in $W(CO)_6$.

We discuss now the results for $Ag(CO)^+$ and $Au(CO)^+$. Table 4 shows that the MP2 optimized $AgCO^+$ bond length is longer (2.329 Å) than experimentally observed (2.10 Å).[44] The difference between theory and experiment is probably due to the coordination of Ag in the solid state, which is tricoordinated rather than monocoordinated. The theoretically predicted Au−CO^+ distance (1.975 Å) is in good agreement with the experimental value for Au(CO)Cl (1.93 Å).[48]

TABLE 6: Charge Components for the Caononical (Natural) MOs of $AgCO^+$ at the HF(MP2) level

orb	occ	*d*	*b*	*r*
1σ	2.0(2.000)	0.000(0.000)	0.000(0.000)	0.000(0.000)
2σ	2.0(2.000)	+0.001(0.000)	0.000(0.000)	0.000(0.000)
3σ	2.0(1.999)	0.000(0.000)	0.000(0.000)	0.000(+0.003)
1π	2.0(1.997)	0.000(0.000)	0.000(0.000)	0.000(0.000)
1π	2.0(1.997)	0.000(0.000)	0.000(0.000)	0.000(0.000)
4σ	2.0(1.997)	0.000(0.000)	+0.001(+0.002)	+0.001(+0.007)
5σ	2.0(1.990)	−0.007(+0.002)	0.000(−0.003)	0.000(−0.007)
6σ	2.0(1.987)	+0.008(+0.032)	0.000(0.000)	+0.006(0.000)
2π	2.0(1.989)	+0.002(0.000)	+0.001(+0.010)	+0.007(+0.001)
2π	2.0(1.989)	+0.002(0.000)	+0.001(+0.010)	+0.007(+0.001)
7σ	2.0(1.965)	+0.080(+0.105)	0.000(+0.001)	+0.163(−0.012)
1δ	2.0(1.990)	0.000(0.000)	0.000(0.000)	0.000(0.000)
1δ	2.0(1.990)	0.000(0.000)	0.000(0.000)	0.000(0.000)
3π	2.0(1.941)	0.000(+0.003)	+0.003(−0.001)	−0.008(−0.003)
3π	2.0(1.941)	0.000(+0.003)	+0.003(−0.001)	−0.008(−0.003)
8σ	2.0(1.971)	+0.164(+0.195)	−0.005(0.000)	−0.213(−0.047)
Σσ		+0.245(+0.328)	−0.005(0.000)	−0.043(−0.058)
Σπ		+0.003(+0.002)	+0.007(+0.016)	−0.002(−0.004)
Σδ		0.000(0.000)	0.000(0.000)	0.000(0.000)
Σ		+0.248(+0.330)	+0.002(+0.016)	−0.045(−0.062)
Σ	TZ2P	+0.216(+0.298)	+0.008(+0.025)	−0.046(−0.061)

TABLE 7: Charge Components for the Canonical (Natural) MOs of $AuCO^+$ at the HF(MP2) Level

orb	occ	*d*	*b*	*r*
1σ	2.0(2.000)	0.000(+0.002)	0.000(0.000)	0.000(+0.001)
2σ	2.0(2.000)	+0.002(0.000)	0.000(0.000)	0.000(0.000)
3σ	2.0(1.999)	0.000(0.000)	−0.002(−0.002)	0.000(+0.012)
4σ	2.0(1.998)	0.000(0.000)	+0.001(+0.003)	+0.005(+0.025)
1π	2.0(1.998)	0.000(0.000)	0.000(0.000)	0.000(0.000)
1π	2.0(1.998)	0.000(0.000)	0.000(0.000)	0.000(0.000)
5σ	2.0(1.986)	−0.020(−0.044)	0.000(+0.005)	−0.001(+0.090)
6σ	2.0(1.965)	−0.008(+0.055)	0.000(0.000)	+0.024(−0.004)
7σ	2.0(1.971)	+0.094(+0.166)	+0.004(−0.013)	+0.181(−0.095)
2π	2.0(1.940)	+0.003(+0.001)	+0.002(−0.004)	+0.019(−0.023)
2π	2.0(1.940)	+0.003(+0.001)	+0.002(−0.004)	+0.019(−0.023)
3π	2.0(1.988)	−0.002(+0.001)	+0.020(+0.055)	−0.026(+0.009)
3π	2.0(1.988)	−0.002(+0.001)	+0.020(+0.055)	−0.026(+0.009)
1δ	2.0(1.991)	0.000(0.000)	0.000(0.000)	0.000(0.000)
1δ	2.0(1.911)	0.000(0.000)	0.000(0.000)	0.000(0.000)
8σ	2.0(1.989)	+0.190(+0.114)	−0.018(+0.001)	−0.333(−0.189)
Σσ		+0.258(−0.280)	−0.015(−0.011)	−0.124(−0.161)
Σπ		+0.002(+0.002)	+0.043(+0.100)	−0.013(−0.029)
Σδ		0.000(0.000)	0.000(0.000)	0.000(0.000)
Σ		+0.260(+0.282)	+0.028(+0.089)	−0.137(−0.190)
Σ	TZ2P	+0.249(+0.266)	+0.051(+0.137)	−0.157(−0.203)

The results of the charge decomposition analysis of $Ag(CO)^+$ and $Au(CO)^+$ are shown in Tables 6 and 7. The calculations suggest that back donation from Ag^+ to CO is negligible. The Ag^+−CO bond is nearly exclusively formed by the σ donation from CO to Ag^+. The calculated donation at the MP2 level for $Ag(CO)^+$ is 0.330 e, while the back donation is only 0.016 e. A somewhat larger M → CO back donation is calculated at the MP2 level for $Au(CO)^+$, but the donation is still much larger (0.282 e) than the back donation (0.089 e). The calculated *d*, *b*, and *r* contributions for $Ag(CO)^+$ change very little when the TZ2P basis set is used instead of 6-31G(d) (Table 6). The back donation of $Au(CO)^+$ is larger at the MP2/TZ2P level (+0.137) than at MP2/6-31G(d), but it is still substantially smaller than the CO → Au^+ donation.

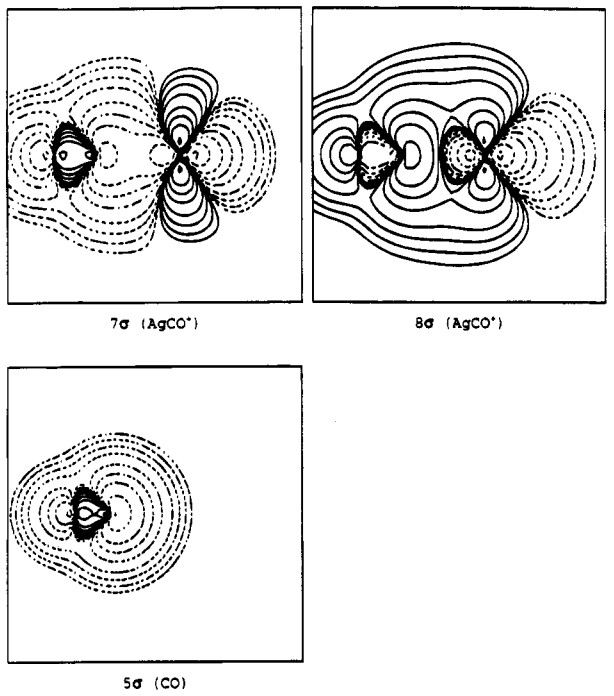

Figure 10. Contour line diagrams of the 7σ and 8σ canonical orbitals of $Ag(CO)^+$ and the 5σ canonical orbital (HOMO) of CO at the HF/6-31G(d) level.

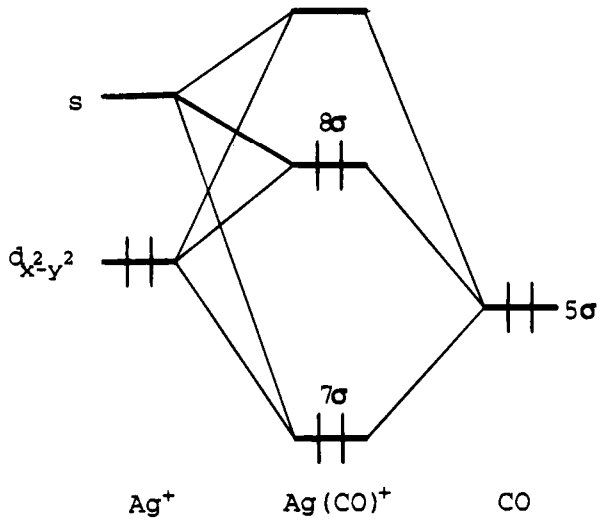

Figure 11. Schematical representation of the interactions between the σ orbitals of CO and Ag^+.

It is interesting to note that there are *two* orbitals, the 7σ and 8σ orbitals, which contribute strongly to the σ-donation in $Ag(CO)^+$ and $Au(CO)^+$ (Tables 6 and 7). Figure 10 shows the contour line diagrams of the 7σ and 8σ canonical orbitals of $Ag(CO)^+$ and the 5σ orbital of CO. It is obvious that the 7σ and 8σ orbitals of $Ag(CO)^+$ are mainly the bonding and antibonding combinations of the CO carbon lone-pair orbital and the $4d_{x^2-y^2}$ AO of Ag^+, with some mixing of the 5s AO. This is schematically shown in Figure 11. The 7σ orbital is the bonding combination, which explains why the occupied/occupied contribution to the canonical orbital is positive (+0.163 e). The 8σ orbital is the antibonding combination. Therefore, the occupied/occupied contribution to the canonical orbital is negative (−0.213 e). The natural orbitals 7σ and 8σ show a cancellation of the occupied/occupied contributions (Table 6). The reason why the interactions between the occupied orbitals 5 σ of CO and $4d_{x^2-y^2}$ of Ag^+ are stabilizing is, that there is some mixing with the empty 5s AO of Ag^+.

Summary

The results of the charge decomposition analysis of the LCFO molecular orbitals show that the CDA method is a valuable tool to analyze quantitatively the interactions between two molecular fragments in terms of donation, and polarization using quantum mechanical ab initio calculations. The results obtained at the HF and MP2 level of theory are fairly invariant to the size of the basis set if at least a DZ+P valence basis set is used. The numerical results of the charge decomposition analysis are in agreement with qualitative models of donor–acceptor complexes and metal-ligand interactions, such as the Dewar–Chatt–Duncanson model. The CDA method indicates strong electron donation from CO to BH_3 and significant back donation from BH_3 to CO in H_3BCO, which is about half the size of the electron donation. There is also strong electron donation from NH_3 to BH_3 in H_3BNH_3, but there is practically no back donation from BH_3 to NH_3. Electron donation and back donation in $W(CO)_6$ have a similar magnitude, while the donation is much higher than the back donation in $Ag(CO)^+$ and $Au(CO)^+$. The CDA method is a promising tool to calculate the relative amount of electron donation and back donation in transition metal complexes for different ligands and different metals. Systematic studies of transition-metal complexes are in progress.

Acknowledgment. This work was supported by the Fonds der Chemischen Industrie and the Deutsche Forschungsgemeinschaft. The authors thank Dr. Alberto Gobbi for valuable discussions. Excellent service by the computer center of the Philipps-Universität Marburg is gratefully acknowledged. Additional computer time was given by the HHLR Darmstadt and the HLRZ Jülich.

References and Notes

(1) Absar, I.; Van Wazer, J. *Angew. Chem.* **1978**, *90*, 86; *Angew. Chem., Int. Ed. Engl.* **1978**, *17*, 80.
(2) Jug, K.; Maksic, Z. B. In *Theoretical methods in chemical bonding*; Maksic, Z. B., Eds.; Springer-Verlag: Berlin, 1991; Part 3, pp 235ff.
(3) Mulliken, R. S. *J. Chem. Phys.* **1955**, *23*, 1833, 1841, 2338–2343.
(4) Löwdin, P. O. *J. Chem. Phys.* **1955**, *21*, 374.
(5) Roby, K. R. *Mol. Phys.* **1974**, *27*, 81.
(6) Mayer, I. *Chem. Phys. Lett.* **1984**, *110*, 440.
(7) Cioslowski, J. *J. Am. Chem. Soc.* **1989**, *111*, 8333.
(8) See, for example: Collins, J. B.; Streitwieser Jr., A. *J. Comput. Chem.* **1980**, *1*, 81.
(9) Davidson, E. R. *J. Chem. Phys.* **1967**, *46*, 3320.
(10) Reed, A. E.; Curtiss, L. A.; Weinhold, F. *Chem. Rev.* **1988**, *88*, 899.
(11) Bader, R. F. W.; Popelier, P. L. A. *Int. J. Quantum. Chem.* **1993**, *45*, 189.
(12) Gatti, C.; Fantucci, P.; Pacchioni, G. *Theor. Chim. Acta* **1987**, *72*, 433.
(13) (a) Dewar, J. S. *Bull. Soc. Chim. Fr.* **1951**, *18*, c79. (b) Chatt, J.; Duncanson, L. A. *J. Chem. Soc.* **1953**, 2939.
(14) (a) Morokuma, K. *J. Chem. Phys.* **1971**, *55*, 1236. (b) Kitaura, K.; Morokuma, K. *Int. J. Quantum. Chem.* **1976**, *10*, 325. (c) Morokuma, K. *Acc. Chem. Res.* **1977**, *10*, 249.
(15) (a) Bagus, P. S.; Hermann, K.; Bauschlicher, C. W. *J. Chem. Phys.* **1984**, *80*, 4378. (b) Bagus, P. S.; Hermann, K.; Bauschlicher, C. W. *J. Chem. Phys.* **1984**, *81*, 1966. (c) Bagus, P. S.; Illas, F. *J. Chem. Phys.* **1992**, *96*, 8962. (d) Inagaki, S.; Goto, N.; Yoshikawa, K. *J. Am. Chem. Soc.* **1991**, *113*, 7144. (e) Inagaki, S.; Yoshikawa, K.; Hayano, Y. *J. Am. Chem. Soc.* **1993**, *115*, 3706. (f) Inagaki, S.; Ishitani, Y.; Kafeku, T. *J. Am. Chem. Soc.* **1994**, *116*, 5954. (g) Ziegler, T.; Rauk, A. *Theor. Chim. Acta* **1977**, *46*, 1. (h) Baerends, E. J.; Rozendaal, A. *NATO ASI* **1986**, *C176*, 159.
(16) Blyholder, G.; Lawless, M. *J. Am. Chem. Soc.* **1992**, *114*, 5828.
(17) Glendening, E. D.; Streitwieser, A. *J. Chem. Phys.* **1994**, *100*, 2900.
(18) (a) Frenking, G.; Heinrich, N. *Theor. Chim. Acta (Berlin)* **1984**, *65*, 65. (b) Frenking, G. *J. Mol. Struct.* **1983**, *104*, 233–239. (c) Frenking, G.; Schmidt, J. *Tetrahedron* **1984**, *40*, 2123.
(19) (a) Fujimoto, H.; Kato, S.; Yamabe, S.; Fukui, K. *J. Chem. Phys.* **1974**, *60*, 572. (b) Kato, S.; Fujimoto, H.; Yamabe, S.; Fukui, K. *J. Am. Chem. Soc.* **1974**, *94*, 2024. (c) Lowe, J. P. *J. Am. Chem. Soc.* **1971**, *93*,

301. Lowe, J. P. *J. Am. Chem. Soc.* **1972**, *94*, 60. (d) Lowe, J. P. *J. Am. Chem. Soc.* **1972**, *94*, 3718. (e) Whangbo, M.-H.; Wolfe, S. *Can. J. Chem.* **1976**, *54*, 949. (f) Whangbo, M.-H.; Schlegel, H. B.; Wolfe, S. *J. Am. Chem. Soc.* **1977**, *99*, 1296.

(20) Löwdin, P.-O. *Phys. Rev.* **1955**, *97*, 1474.

(21) Concerning the supermolecule approach, see: (a) Maitland, G. C.; Rigby, M.; Smith, E. B.; Wakeham, W. A. *Intermolecular forces*; Oxford University Press: Oxford, 1981. (b) Hobza, P.; Zahradnik, R. *Intermolecular complexes. The role of van der Waals systems in physical chemistry and in the biodisciplines*; Elsevier: Amsterdam, 1988.

(22) Boys, S. F.; Bernardi, F. *Mol. Phys.* **1970**, *19*, 553.

(23) Hehre, W. J.; Ditchfield, R.; Pople, J. A. *J. Chem. Phys.* **1972**, *56*, 2257.

(24) Huzinaga, S. *Approximate Atomic Wavefunctions*; Department of Chemistry Report, University of Alberta; Edmonton, Alberta, Canada, 1971. TZ2P for B, C, and N is a (9s5p2d)/[5s3p2d] basis set, TZ2P for H is a (5s2p)/[3s2p] basis set.

(25) Binkley, J. S.; Pople, J. A.; Hehre, W. J. *J. Am. Chem. Soc.* **1980**, *102*, 939.

(26) Krishnan, R.; Binkley, J. S.; Seeger, R.; Pople, J. A. *J. Chem. Phys.* **1980**, *72*, 650.

(27) CDA 1.0, Dapprich, S.; Frenking, G., Marburg, 1994. Internet: ftp.chemie.uni-marburg.de, login anonymous, directory pub/cda.

(28) Gaussian 92, Revision C, Frisch, M. J.; Trucks, G. W.; Head-Gordon, M.; Gill, P. M. W.; Wong, M. W.; Foresman, J. B.; Johnson, B. G.; Schlegel, H. B.; Robb, M. A.; Replogle, E. S.; Gomperts, R.; Andres, J. L.; Raghavachari, K.; Binkley, J. S.; Gonzalez, C.; Martin, R. L.; Fox, D. J.; Defrees, D. J.; Baker, J.; Stewart, J. J. P.; Pople, J. A. Gaussian, Inc.: Pittsburgh, PA, 1992.

(29) Hay, P. J.; Wadt, W. R. *J. Chem. Phys.* **1985**, *82*, 299.

(30) Ehlers, A. W.; Böhme, M.; Dapprich, S.; Gobbi, A.; Höllwarth, A.; Jonas, V.; Köhler, K. F.; Stegmann, R.; Veldkamp, A.; Frenking, G. *Chem. Phys. Lett.* **1993**, *208*, 111.

(31) Roeggen, I. *Chem. Phys.***1994**, *100*, 2900.

(32) Mulliken, R. S. *J. Am. Chem. Soc.* **1950**, *72*, 600.

(33) Hanna, M. W. *J. Am. Chem. Soc.* **1968**, *90*, 285.

(34) Mulliken, R. S.; Person, N. B. *J. Am. Chem. Soc.* **1969**, *91*, 3409.

(35) (a) Morokuma, K. *Acc. Chem. Res.* **1977**, *10*, 294. (b) Umeyama, H.; Morokuma, K. *J. Am. Chem. Soc.* **1976**, *98*, 7208.

(36) Jonas, V.; Frenking, G.; Reetz, M. T. *J. Am. Chem. Soc.* **1994**, *116*, 8741.

(37) (a) Hughes, E. W. *J. Am. Chem. Soc.* **1956**, *78*, 502. (b) Lippert, E. L.; Lipscomb, W. N. *Ibid.* **1956**, *78*, 503.

(38) (a) Davidson, E. R.; Kunze, K. L.; Machado, F. B.; Chakravorty, S. J. *Acc. Chem. Res.* **1993**, *26*, 628. (b) Bauschlicher, C. W., Jr.; Bagus, P. S. *J. Chem. Phys.* **1984**, *81*, 5889. (c) Bagus, P. S.; Nelin, C. J.; Bauschlicher, C. W. *J. Vac. Sci. Technol.* **1984**, *A2*, 905. (d) Bauschlicher, C. W., Jr.; Bagus, P. S.; Nelin, C. J.; Roos, B. O. *J. Chem. Phys.* **1986**, *85*, 354. (d) Koutecky, J.; Pacchioni, G.; Fantucci, P. *Chem. Phys.* **1985**, *99*, 87. (e) Hermann, K.; Bagus, P. S.; Nelin, C. J. IBM Research Report No. RJ 05361 (55070); IBM: Tarrytown, NY, 1986. (f) Muller, W.; Bagus, P. S. *J. Vac. Sci. Technol.* **1985**, *A3*, 1623. (g) Hermann, K.; Bagus, P. S. *Phys. Rev.* **1977**, *B16*, 4195. (h) Baerends, E. J.; Rozendaal, A. In *Quantum Chemistry: The Challenge of Transition Metals and Coordination Chemistry*; Veillard, A., Ed.; D. Reidel: Dordrecht, Holland, 1986.

(39) Jones, L. H. *Spectrochim. Acta* **1963**, *19*, 329.

(40) Herzberg, G. *Spectra of Diatomic Molecules*, 2nd ed.; D. Van Nostrand: New York, 1950.

(41) (a) Hurlburt, P. K.; Rack, J. J.; Luck, J. S.; Dec, S. F.; Webb, J. D.; Anderson, O. P.; Strauss, S. H. *J. Am. Chem. Soc.* **1994**, *116*, 10003. (b) Strauss, S. H. *Chem. Rev.* **1993**, *93*, 927. (c) Hurlburt, P. K.; Rack, J. J.; Dec, S. F.; Anderson, O. P.; Strauss, S. H. *Inorg. Chem.* **1993**, *32*, 373. (d) Hurlburt, P. K.; Anderson, O. P.; Strauss, S. H. *J. Am. Chem. Soc.* **1991**, *113*, 6277.

(42) (a) Willner, H.; Schaebs, J.; Hwang, G.; Mistry, F.; Jones, R.; Trotter, J.; Aubke, F. *J. Am. Chem. Soc.* **1992**, *114*, 8972. (b) Hwang, G.; Bodenbinder, H.; Willner, H.; Aubke, F. *Inorg. Chem.* **1993**, *32*, 4667.

(43) (a) Belli Dell'Amico, D.; Calderazzo, F.; Robino, P.; Serge, A. *Gazz. Chim. Ital.* **1991**, *121*, 51; *J. Chem. Soc., Dalton Trans.* **1991**, 3017. (b) Belli Dell'Amico, D.; Calderazzo, F.; Dell'Amico, G. *Gazz. Chim. Ital.* **1977**, *107*, 101. (c) Calderazzo, F. *Pure Appl. Chem.* **1978**, *50*, 49. (d) Browning, J.; Goggin, P. L.; Goodfellow, R. J.; Norton, M. J.; Rattray, A. J. M.; Taylor, B. F.; Mink, J. *J. Chem. Soc., Dalton Trans.* **1977**, 2061. (e) Willner, H.; Aubke, F. *Inorg. Chem.* **1990**, *29*, 2195. (f) Weber, L. *Angew. Chem.* **1994**, *106*, 1131; *Angew. Chem., Int. Ed. Engl.* **1994**, *33*, 1077.

(44) Veldkamp, A.; Frenking, G. *Organometallics* **1993**, *12*, 4613.

(45) (a) Pepin, C.; Lambert, L.; Cabana, A. *J. Mol. Spectrosc.* **1974**, *53*, 120. (b) Vencatachar, A. C.; Taylor, R. C.; Kuczkowski, R. L. *J. Mol. Struct.* **1977**, *38*, 17. (c) Lias, S. G.; Bartmess, J. E.; Liebman, J. F.; Holmes, J. L.; Levin, R. D.; Mallard, W. G. *J. Phys. Chem. Ref. Data* **1988**, *17*, Suppl. 1.

(46) (a) Thorne, L. R.; Suenram, R. D.; Lovas, F. J. *J. Chem. Phys.* **1983**, *78*, 167. (b) Haaland, A. *Angew. Chem.* **1989**, *101*, 1017; *Angew. Chem., Int. Ed. Engl.* **1989**, *28*, 992.

(47) Jost, A.; Rees, B. *Acta Crystallogr.* **1975**, *B31*, 2649.

(48) Jones, P. G. Z. *Naturforsch.* **1982**, *37b*, 823.

JP9432556